Journal of Macromolecular Science, Part A
Publication details, including instructions for authors and subscription information:
http://www.informaworld.com/smpp/title~content=t713597274

Effect of Active Filler Addition on the Ionic Conductivity of PVDF-PEG Polymer Electrolyte

Yun-Pu Wang[a]; Xiang-Hu Gao[a]; Hong-Kun Li[a]; Hong-Jun Li[a]; Han-Gong Liu[b]; Hui-Xia Guo[a]
[a] Institute of Polymer, Key Laboratory of Polymer Materials of Gansu Province, Northwest Normal University, Lanzhou, China [b] Gansu Research Institute of Chemical Industry, Lanzhou, Gansu, China

To cite this Article Wang, Yun-Pu , Gao, Xiang-Hu , Li, Hong-Kun , Li, Hong-Jun , Liu, Han-Gong and Guo, Hui-Xia(2009) 'Effect of Active Filler Addition on the Ionic Conductivity of PVDF-PEG Polymer Electrolyte', Journal of Macromolecular Science, Part A, 46: 4, 461 — 467
To link to this Article: DOI: 10.1080/10601320902740277
URL: http://dx.doi.org/10.1080/10601320902740277

Journal of Macromolecular Science®, Part A: Pure and Applied Chemistry (2009) **46**, 461–467

ISSN: 1060-1325 print / 1520-5738 online
DOI: 10.1080/10601320902740277

Taylor & Francis
Taylor & Francis Group

Effect of Active Filler Addition on the Ionic Conductivity of PVDF-PEG Polymer Electrolyte

YUN-PU WANG[1]*, XIANG-HU GAO[1], HONG-KUN LI[1], HONG-JUN LI[1], HAN-GONG LIU[2] and HUI-XIA GUO[1]

[1]*Institute of Polymer, Key Laboratory of Polymer Materials of Gansu Province, Northwest Normal University, Lanzhou 730070, China*
[2]*Gansu Research Institute of Chemical Industry, No.1 Guchengping, Lanzhou 730020, Gansu, China*

Received July 2008; Accepted October 2008

A novel composite microporous polymer electrolyte based on poly(vinylidene fluoride), PVDF, poly(ethylene glycol), PEG, and Li-exchanged vermiculite(Li-VMT)was prepared by a simple phase inversion technique. The prepared membrane was subjected to XRD, SEM, impedance spectroscopy. The incorporation of Li-exchanged vermiculite greatly enhanced the ionic conductivity and solvent uptake as compared to the membrane without Li-exchanged vermiculite. The Li-exchanged vermiculite plays a active role in ion transport since relatively large platelets serve as the anion and allowed for exceptionally large Li transference numbers.

Keywords: Active fillers, Polymer electrolyte, PVDF, PEG, Vermiculite

1 Introduction

The science of polymer electrolytes is a highly specialized interdisciplinary field which encompasses the disciplines of electrochemistry, polymer science, organic chemistry, and inorganic chemistry. The field has attracted ever-increasing interest, both in academia and industry, for the past two decades due to the potentially promising applications in all solid-state rechargeable lithium or lithium-ion batteries. Many microporous polymer electrolytes comprising polymer matrices, plasticizing organic solvents and alkali metal salts have been intensively studied for applications in rechargeable lithium batteries and other electrochemical devices (1). Microporous polymer electrolytes in the form of very thin films act simultaneously as transport for lithium ions, separator, and binder between the negative (anode) and positive (cathode) electrodes. Although gel polymer electrolytes with high ionic conductivity can usually be achieved by adding large amounts of organic solvents, they do not have sufficient mechanical ruggedness to withstand winding and stacking during manufacturing, or the stress that arises from morphological deformation of the electrode during repeated charge–discharge (2–4). Various approaches to increasing the mechanical strength have been proposed recently. Inorganic fillers, such as fume silica, zeolite, clay, Al_2O_3or glass fiber have been added to strengthen the dimensional stability of gel polymer electrolytes (5–7). Missing, however, is a detailed analysis of the contribution to ionic conductivity of different fillers.

A related approach to improve the performance of polymer electrolyte by enhancing the Li transference number uses Li-exchanged vermiculite in PEO capable of solvating Li cations (8–10). In this regard, PEG molecules intercalate within the galleries of the clay platelets and solvate the Li cations. The large clay platelets therefore serve as anions, but have low mobility because of their size. As such, high Li transference numbers can be expected. Since the Li-exchanged vermiculite used in this systems directly affected ion transport, we refer to them as active fillers.

In the present paper, we report the preparation and characterization of microporous PVDF–PEG polymer electrolytes with active filler (Li-VMT). The prepared membrane was subjected to XRD, SEM, impedance spectroscopy. Li-exchanged vermiculite constitutes an active filler that benefits Li transference number. The solvent uptake and ionic conductivity were also discussed.

*Address correspondence to: Yun-Pu Wang, Institute of Polymer, Key Laboratory of Polymer Materials of Gansu Province, Northwest Normal University, Lanzhou 730070, China. E-mail: gaoxh121@163.com

2 Experimental

2.1 Materials

PVDF (Mw = 900,000) was obtained from Shanghai 3F New Material Co., LTD and dried in a vacuum oven at 100°C for 48 h before use. PEG (Mw = 10,000) and LiCl were purchased from Shanghai Pudong Chemical Company. The ES-002 electrolyte solution (EC: DMC: EMC /1:1:1/ v/v/v 1 M $LiPF_6$) was purchased from Shanghai Tuer Industry Development Co., LTD. Conductivity of this electrolyte is 9.9 mS cm^{-1}. The vermiculite used in this work was grade number 3, purchased from Aldrich and treated at 120°C for 6 h prior to use. Other chemicals were obtained from commercial suppliers and used without further purification.

2.2 Preparation of Li-Exchanged Vermiculite

Li-exchanged vermiculite (Li-VMT) was made by cation exchange in 1 M aqueous LiCl solution and by using enough solution to provide a 10-fold excess of cation needed for complete exchange. The exchange suspensions were stirred for 2 h at room temperature and then were centrifuged, and the process was repeated twice. The samples were then washed with distilled water (suspended in water and centrifuged) until the product was chloride-free as tested using 10^{-1}M $AgNO_3$ solution.

2.3 Preparation of Composite Microporous Membranes

The PVDF–PEG/Li-VMT composite microporous membranes were prepared by a solution cast method. All percentages for the additives were normalized with respect to the weight of the polymer. Typically, a procedure involved 1 wt% Li-VMT loading was prepared as following. First, Li-VMT (0.02 g) powder was introduced into 10 ml of DMF solution with stirring for 12 h at RT. PVDF (1 g) and PEG (1 g) powders were added to DMF solution (20 ml) in another glass bottle with stirring for 12 h at 80°C. Second, the clay solution was mixed with the polymer solution with shear supplied via sonication for 24 h at 60°C. The resulted viscous slurry was cast onto a glass substrate using a doctor blade and slowly dried at 100°C, until a uniform and freestanding membranes was obtained. This procedure yielded mechanically stable, free standing films of thickness ranging from 100 to 300 μm. TG analysis confirmed that both solvent and non-solvent evaporated completely during the above preparation process. The same procedure was also employed for the preparation of PVDF-PEG/0 wt% Li-VMT polymer electrolyte.

2.4 Characterization

Wide angle X-ray diffraction (WXRD) with a Rigaku D/max-2400 diffractometer (CuKa radiation = 0.15 nm, generator voltage = 40 kV, current = 60 mA) was used in this work. The microstructure of these hybrid nanocomposites was imaged using Hitachi H-600 equipment, TEM samples of nanoparticles were prepared by casting one drop of a dilute colloid solution onto a carbon-coated copper grid.

Pore distribution and pore structure in the surface and bulk of PVDF-PEG/Li-VMT composite microporous membranes were studied by scanning electron microscopy (SEM) using a Field Emission Scanning Electron Microscope (JSM-6701F) with gold sputtered coated films. To observe the cross-section of the samples, the membranes were broken in liquid nitrogen.

The liquid electrolyte uptake of composite microporous membranes was measured in a simple glove box. The electrolyte membrane was cut into a disk with a diameter of 1 cm. After the mass (w_0) of the membrane disk was measured, it was soaked in ES-002 electrolyte solution for a period of time to obtain the wetted polymer electrolyte. After the remaining solution at the surface of the wetted polymer electrolyte membrane was absorbed with filter paper, the membrane was weighed (w_t). In this study, the ES-002 solution uptake was calculated by the following Equation 1:

$$\text{Weight uptake } (\%) = 100 \times (w_t - w_0)/w_0 \qquad (1)$$

Where w_t and w_0 are the weight of the wet and dry membrane, respectively.

The ionic conductivity of the polymer electrolyte was determined by AC impedance spectroscopy at room temperature. The samples were sandwiched between stainless steel blocking electrodes. The impedance measurements were carried out on an Automatic Component Analyzer(TH2818) with a frequency range of 20–300 KHz. The ionic conductivity (σ) was then calculated from the electrolyte resistance (R_b) obtained from the intercept of the Nyquist plot with the real axis, the membrane thickness (l), and the electrode area (A) according to the equation:

$$\sigma = 1/AR_b.$$

3 Results and Discussions

3.1 SEM and XRD Analysis

Vermiculite (VMT), a mica-type silicate, possesses a layered structure. Each layer consists of octahedrally coordinated cations (typically Mg, Al, and Fe) sandwiched by tetrahedrally coordinated cations (typically Si and Al). The isomorphous substitution of Si^{4+} by Al^{3+} leads to a net negative surface charge that is compensated by an interlayer of exchangeable hydrated cations (Ca^{2+}, Mg^{2+}, Cu^{2+}, Na^{+}, and H^{+}). Figure 1 shows the SEM image of VMT. The structure of as-received VMT exhibits a more ordered character. It can be seen that the flakes are remarkably compact

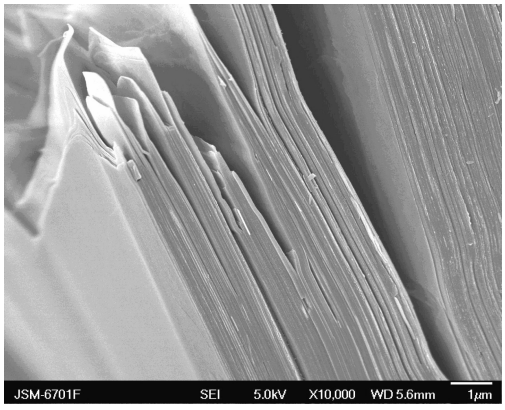

Fig. 1. SEM image of as-received Vermiculite.

and gaps between them are smaller and not torn on the edges.

Due to the fine particle, the low crystallizability, and the complicated chemical components of clays, detailed information about the interlayer structure and the atomic local environment in organoclay is rarely available from experimental measurements. So far, X-ray diffraction (XRD) is the most widely used technique to determine the structure of organoclays (11). The structure and apparent interlayer spacing (*d* spacing) of the VMT and Li-VMT have been detected. Figure 2 shows the XRD patterns for the as-received VMT, Li-VMT and PVDF-PEG/Li-VMT nanocomposites. As-received VMT yields characteristic diffraction peaks at $2\theta = 3.2°$, 7.0°, and 8.4°. The diffraction peaks at $2\theta = 7.0°$ ($d_{001} = 1.254$ nm) represents the interlayer spacing of VMT, while the broad peak at $2\theta = 3.2°$ is also d_{001} of the VMT intercalated by other impurities, such as the water. The diffraction peak at $2\theta = 8.4°$ probably resulted from the impurities within VMT. Under ambient conditions of relative humidity, the basal spacing of VMT and Li-VMT are 1.254 and 1.135 nm, respectively. This change tendency is agreed with previous report as compared to montmorillonite (12).

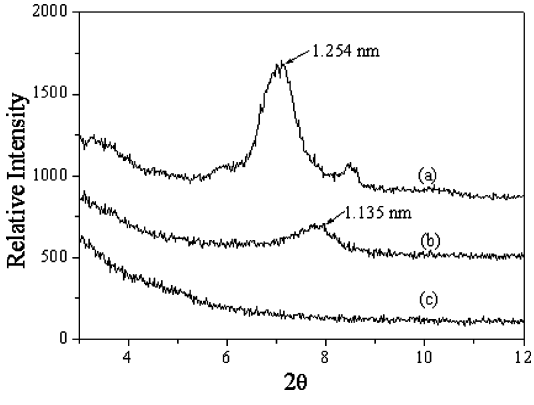

Fig. 2. XRD patterns of: (a) as-received vermiculite; (b) Li-VMT; (c) PVDF-PEG/1 wt% Li-VMT.

Generally speaking, there are two terms used to describe the prepared polymer/clay nanocomposite: intercalated and delaminated nanocomposite. In the intercalated structures case, the VMT clays sustain the self-assembled, well order multi-layer structures. The extended polymer chains are inserted into the gallery space between parallel individual silicates layers. In the delaminated structures case, the interlayer spacing can be on the order of the radius of gyration of the polymer. The individual silicate layers are no longer close enough to interact with the adjacent layers' gallery cations when the delaminated (or exfoliated) structures could be obtained. Therefore, the silicate layers may be considered to disperse in the organic polymer. Upon further intercalation of PVDF and PEG, there is no diffraction peak observed in the WAXD trace (Figure 2c). This indicated that most of the Li-VMT sheets were dispersed uniformly in the polymer matrix in nanoscale. Exfoliated polymer/clay nanocomposites are especially desirable for improved properties because of their large aspect ratio, the homogeneous dispersion of clay, and the large interfacial area (and consequently, strong interaction) between polymer chains and clay nanolayers.

3.2 TEM Analysis

XRD analysis alone is not enough to interpret the extent of the exfoliation. Thus, TEM studies are necessary to verify the extent of exfoliation achieved. As presented in Figure 3, the stacks of VMT sheets were dispersed within the PVDF-PEG matrix irregularly. It can be seen that some of VMT layers were intercalated and dispersed perpendicularly to the sample surface within the PVDF-PEG matrix, while some VMT sheets were parallel to the surface of the nanocomposites slice. Intercalated layers of Li-VMT were dispersed homogeneously in the PVDF-PEG matrix, however, a small amount of unexfoliated Li-VMT layers existed as clusters as shown in Figure 3. In this sense, the PVDF-PEG /Li-VMT nanocomposites is considered to be a mixed delaminated/intercalated system. The existence of

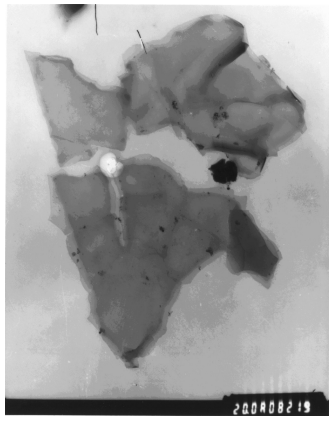

Fig. 3. TEM photographs of PVDF-PEG/1 wt% Li-VMT.

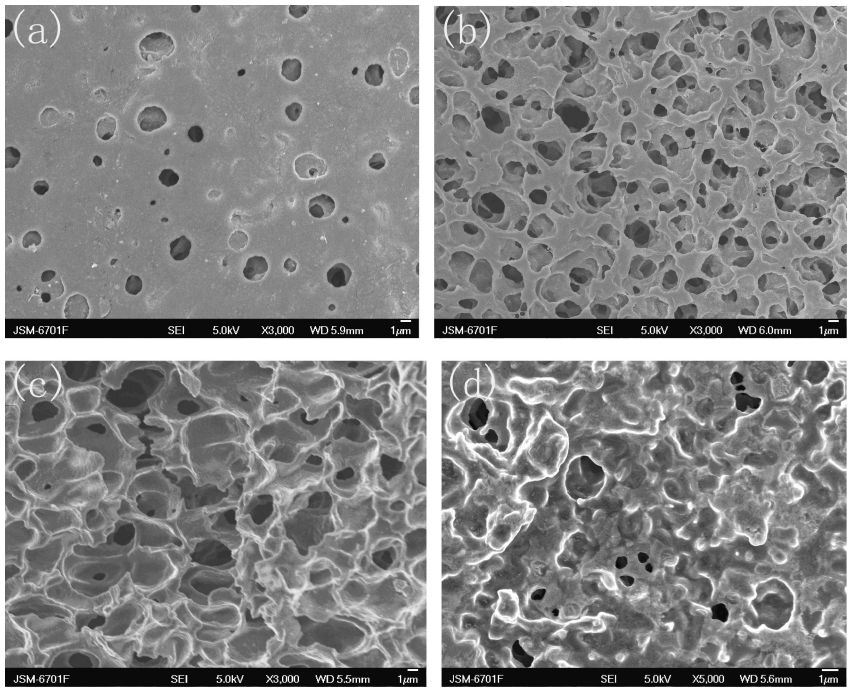

Fig. 4. SEM images of polymer membrane and the gels after immersion in the mixed electrolyte: (a) bottom surface; (b) top surface; (c) cross-section; (d) gel of polymer membrane.

the obstacle peaks in the XRD patterns of the nanocomposite (trace c of Figure 2) was believed to be attributed these unexfoliated clusters.

3.3 The Morphology of the PVDF-PEG/1wt% Li-VMT Polymer Membrane

It has been reported that morphology of the film cast from solution is influenced by polymer–solvent complex formation, solution preparation temperature, solvating power, solvent evaporation temperature, and solvent evaporation rate (13–15). Polymer–solvent complex formation affects the polymer conformation; if the solvent molecules disrupt the dipole and van der Waals interactions that hold the polymer chains together, polymer chains become more disentangled. Therefore, increased polymer–solvent complexation gives a rough surface. The pore structure is usually controlled by the phase inversion process and is discussed in terms of the liquid–liquid phase separation such as nucleation-growth and spinodal decomposition (16–18).

It is well known that during the coating process, there is always one surface of the membrane facing the air, while the other one faces the substrate. Thus, these two surfaces may differ in morphology to some extent. Usually, the surface facing the air looks rough whereas the surface facing the substrate appears smoother as shown in Figure 4 (a). Figure 4 (b) presents SEM images of the top surface of PVDF-PEG/Li-VMT membranes. It can be seen that the formed membrane exhibits an asymmetric morphology. Those cellular pores are largely independent and are embedded in a continuous polymer matrix. Figure 4 (c) shows the cross-section SEM micrographs of polymer films. It is worth noting that the honeycomb structure is different from the fingerlike structure, in which channels of different sizes are separated by layers of discrete polymer globules (19). Figure 4 (d) shows the surface morphology of the polymer membrane after immersion. It is worth to note that many small pores disappear as compared to Figure 4 (b). This result may contribute to the swelling of polymer.

In this experiment, the solvent DMF has a C=O functional group, which is the main factor for polymer–solvent interaction via the interaction of the C=O dipole with the CH_2CF_2dipole or by limited hydrogen bonding. In addition, rapid solvent evaporation in thin blend films, which can cause significant trapped chain entanglement, leads to a rather homogeneous distribution. It has been reported that the dispersed clay layers act as the nucleation agents in PVDF matrix. A great number of nuclei generated from the nucleation agent simultaneously grow in a limited space and lead to the formation of small spherulites. In addition, the large number of nuclei centers will also cause more crystalline defects and destroy the spherulitic structure. There is a strong interaction between clay and PVDF. The nanometer-size clay layers not only act as nucleating agents and confine the movement of molecular chains and segments but also cause the change of crystalline structure. The results can be attributed to strong interaction at the

interface of PVDF and clay, which confines the movement of molecular chains and segments, resulting in the imperfection of crystals (20).

3.4 Weight Uptake

The PVDF-PEG/Li-VMT nanocomposites exhibit very good film formation and dimensional stability. Most importantly, the membrane containing the exfoliated Li-VMT shows excellent wettability with the electrolyte solution, owning to the high surface area of the silicates layers and good affinity of PVDF to the organic electrolyte solution. The solvent uptake of polymer membrane containing the exfoliated Li-VMT increases largely comparing with those without the filler in the same time scale. Figure 5 presents the solvent uptake percentage of the different films as the function of time, which is used to adsorb the solvent. The percentage can be calculated according to Equation 1. The results illustrate the percentage increases to nearly 35 wt% in 4 h for the membranes containing the exfoliated Li-VMT. At first part the curve is linear as illustrated in Figure 5, which has the characteristic of Fickian diffusion (21). As the swelling ratios increasing, the diffusion becomes anomalous, and the curve shape becomes sigmoidal. The result suggests that Li-VMT facilitates solvent uptake. The solvent uptake percentage of these polymer membranes was fixed by control of the immersing time.

Considering the SEM images (Figure 4 (d)) and weight uptake (Figure 5), we may think that the gel formation process is composed of two distinct steps. First, the solution would mainly enter into the cavities which are present in the porous host polymer because this process provides the lowest energy barrier for the solution flow from outside [initial state]. In the next step, the temporarily trapped solution in the cavities penetrates into the polymer chains to produce saturation. Finally, the gel, the fully swollen polymer reaches an equilibrium condition which provides the maximum conductivity [equilibrium state].

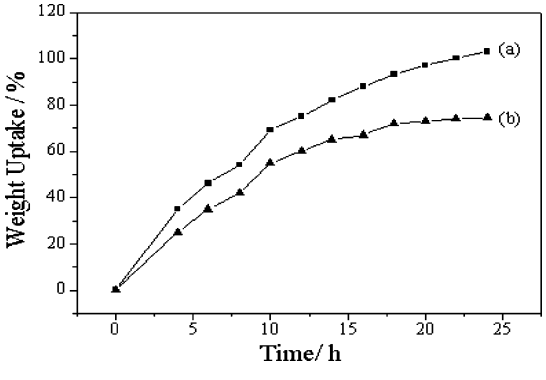

Fig. 5. The relationship of weight uptake percentage vs. time for the polymer membranes with (a) 1 wt% Li-VMT and, (b) without Li-VMT.

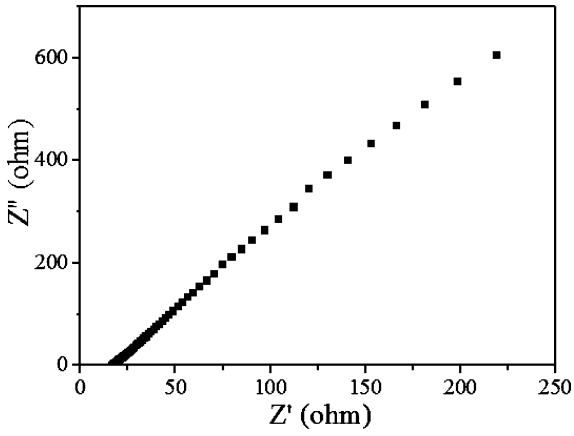

Fig. 6. Typical ac-impedance spectra for PVDF-PEG/1wt% Li-VMT.

3.5 Conductivity

The ionic conductivity (σ) was then calculated from the electrolyte resistance (R_b) obtained from the intercept of the Nyquist plot with the real axis, the membrane thickness (l), and the electrode area (A) according to the equation $\sigma = l/AR_b$. Impedance data are presented in the form of imaginary, Z' (capacitive) against real, Z' (resistive). Figure 6 displays the typical impedance plots (Z', vs. Z''), it can be seen that the entire semicircular portion in the complex impedance representation measured at room impedance plots was disappeared, led to a conclusion that the total conductivity is mainly the result of ion conduction. This phenomena is quite reasonable since the facile mobility in liquid and gel-type electrolyte systems, when compared with solid polymer electrolytes, indicates that ions possess dielectric relaxation times and hence, the inconsequential capacitive effect of the bulk electrolyte in the spectrum (22).

In this experiment, the maximum conductivity (4.2 $mS \cdot cm^{-1}$) was obtained after 20 h immersing in the mixed electrolyte at room temperature.

The affinity between lithium salts and PVDF-based polymer is very poor, so polar solvent (or plasticizer) should be added in gel polymer electrolytes systems (23). EC, EMC and DMC were used in this work based upon their boiling point, viscosity, and dielectric constant. The corresponding liquid electrolyte has an ionic conductivity at around 9.9 mS cm^{-1} at RT. The nanocomposite polymer electrolytes with exfoliated Li-VMT show relatively high ionic conductivity as compared to the polymer electrolyte without Li-VMT. Carrier migration in the porous structure can be restricted because of the convoluted transport pathways that comprise interconnected pores. The restricted condition in

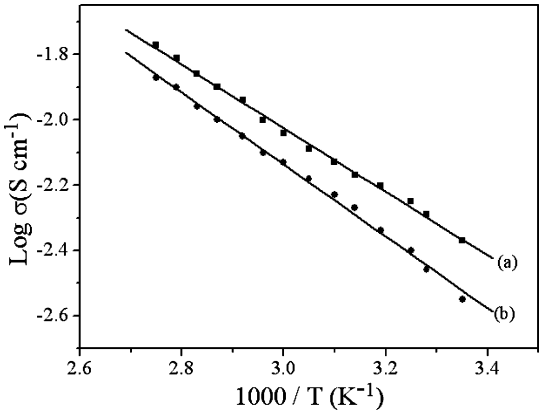

Fig. 7. Arrhenius plots of: (a) PVDF-PEG/1 wt% Li-VMT; (b) PVDF-PEG/0 wt% Li-VMT polymer electrolyte.

migration is affected by pore size, porosity, pore linking condition, and chemical effect of the porous medium on the carriers (24). Detailed carrier diffusivity mechanism in porous membrane is beyond the scope of current work. The images provided in Figure 3 confirm that most of the Li-VMT platelets are intercalated, rather than exfoliated. The extent to which the platelets are intercalated or exfoliated is expected to play a distinct role in the conductivity of these nanocomposites. A completely exfoliated morphology is expected to yield the highest conductivity since more Li cations would be mobile and available for conduction. Conversely, a system in which the Li cations are trapped between intercalated platelets would not be nearly as conductive. In this case, the electronegative silicate platelets in the nanocomposite with high dielectric constant could help to dissolve electrolyte salt, and then increase the ion conduction.

Figure 7 shows an Arrhenius plot of PVDF-PEG polymer electrolyte. It is quite obvious from the figure that the ionic conductivity of polymer electrolyte increases with increase in temperature. Nevertheless, the ionic conduction mainly depends on the entrapped liquid phase in a fully interconnected pore structure and the gel phase. The fact that the conductivity perfectly follows a VTF behavior implies that the motion of the charged species, anions and cations, is controlled by the viscous properties of the mixed electrolyte. These curves appear linear, so the apparent activation energy for the ions transport (Ea) are obtained using the Arrhenius model $\sigma = \sigma^0 \exp(-E\mathrm{a}/RT)$, where R, T, σ and σ^0 are gas constant, temperature, the ionic conductivity of PVDF-PEG polymer electrolyte and the pre-exponential factor, respectively. The activation energy values Ea are 21.71 and 19.1 kJ/mol for the polymer electrolyte membranes with 0% and 1% Li-vermiculite, respectively. The results suggest that the exfoliated Li-VMT have significant effect on the ion transportation activation energy, which is related to the ionic conductivity.

4 Conclusions

This work reported a polymer electrolyte based on poly(vinylidene fluoride), poly(ethylene glycol), and Li-exchanged vermiculite. The polymer electrolyte membrane exhibits good film formation, solvent maintaining capability. After gelling with liquid electrolyte solution (for example, EC: DMC:EMC/1:1:1/ v/v/v 1 M $LiPF_6$), the PVDF-PEG/1wt% Li-VMT polymer electrolyte shows higher ionic conductivity as compared to PVDF-PEG/0 wt% Li-VMT polymer electrolyte. The incorporation of Li-exchanged vermiculite greatly enhanced the ionic conductivity and solvent uptake as compared to the membrane without Li-exchanged vermiculite. The Li-exchanged vermiculite plays a active role in ion transport since relatively large platelets serve as the anion and allowed for exceptionally large Li transference numbers.

Acknowledgments

The project was supported by the Key Laboratory of Eco-Environment-Related Polymer Materials, NCET of Ministry of Education of China.

References

1. Wang, Y.-P., Gao, X.-H., Wang, R.-M., Liu, H.-G., Yang, C. and Xiong, Y.-B. (2008) *React. Funct. Polym.*, 68, 1170–1177.
2. Song, J.Y., Wang, Y.Y. and Wan, C.C. (1999) *J. Power Sour.*, 77, 183–197.
3. Kim, S.H., Cho, J.K. and Bae, Y.C. (2001) *J. Appl. Polym. Sci.,* 81, 948–956.
4. Yarovoy, Y.K., Wang, H.P. and Wunder, S.L. (1999) *Solid State Ionics*, 118, 301–310.
5. Fan, J., Raghavan, S.R., Yu, X.Y., Khan, S.A., Fedkiw, P.S., Hou, J. and Baker, G.L. (1998) *Solid State Ionics*, 111, 117–123.
6. Appetecchi, G.B., Romagnoli, P. and Scrosati, B. (2001) *Electrochem. Commun.*, 3, 281–284.
7. Chen, H.W. and Chang, F.C. (2001) *Polymer*, 42, 9763–9769.
8. Doeff, M.M. and Reed, J.S (1998) *Solid State Ionics*, 113, 109–115.
9. Krawiec, W., Scanlon, L.G., Fellner, J.P., Vais, R.A., Vasudevan, S. and Giannelis, E.P. (1995) *J. Power Sources*, 54, 310–315.
10. Wong, S., Vais, R.A., Giannelis, E.P. and Zax, D.B. (1996) *Solid State Ionics*, 86, 547–557.
11. Yui, T., Yoshida, H., Tachibana, H., Tryk, D.A. and Inoue, H. (2002) *Langmuir,* 18(3), 891–896.
12. Reinholdt, M.X., Kirkpatrick, R.J. and Pinnavaia, T.J. (2005) *J. Phys. Chem. B.*, 109(34), 16296–16303.
13. Benz, M., Euler, W.B. and Gregory, O.J. (2001) *Langmuir*, 17, 239–243.
14. Barnes, M.D., Ng, K.C., Fukui, K., Sumpter, B.G. and Noid, D.W. (1999) *Macromolecules*, 32, 7183–7189.
15. Young, T.H., Huang, J.-H. and Chuang, W.-Y. (2002) *Eur. Polym. J.*, 38, 63–72.
16. Young, T.H., Lin, D.-T., Chen, L.-Y., Huang, Y.-H. and Chiu, W.-Y. (1999) *Polymer*, 40, 5257–5264.

17. Young, T.H., Lai, J.-Y., You, W.-M. and Cheng, L.-P. (1997) *J. Membr. Sci.,* 128, 55–65.
18. Boom, R.M., Wienk, I.M., van den Boomgaard, Th. and Smolders, C.A. (1992) *J. Membr. Sci*., 73, 277–292.
19. Quartarone, E., Mustarelli P. and Magistris A. (2002) *J. Phys. Chem. B*, 106(42), 10828–10833.
20. Yu, W., Zhao, Z., Zheng, W., Song, Y., Li, B., Long, B. and Jiang, Q. (2008) *Mater. Lett*., 62, 747–750.
21. Saunier, J., Alloin, F., Sanchez, J.Y. and Barrière, B. (2004) *J. Polym. Sci. Part B*, 42, 532–543.
22. Song, J.Y., Wang, Y.Y. and Wan, C.C. (2000) *J. Electrochem. Soc*., 147(9), 3219–3225.
23. Wang, M., Zhao, F. and Dong, S. (2004) *J. Phys. Chem. B*, 108, 1365–1370.
24. Saito, Y., Hirai, K., Emori, H., Murata, S., Uetani, Y. and Kii, K. (2004) *J. Phys. Chem. B*, 108(3), 1137–1142.